nature genetics

Article

https://doi.org/10.1038/s41588-024-01943-z

A regulatory network controlling developmental boundaries and meristem fates contributed to maize domestication

Received: 26 September 2023

Accepted: 9 September 2024

Published online: 16 October 2024

Check for updates

Zhaobin Dong 1.2, Gaoyuan Hu1, Qiuyue Chen 3, Elena A. Shemyakina2, Geeyun Chau 12, Clinton J. Whipple 4, Jennifer C. Fletcher 2& George Chuck © 2 2

During domestication, early farmers selected different vegetative and reproductive traits, but identifying the causative loci has been hampered by their epistasis and functional redundancy. Using chromatin immunoprecipitation sequencing combined with genome-wide association analysis, we uncovered a developmental regulator that controls both types of trait while acting upstream of multiple domestication loci. tasselsheath4 (tsh4) is a new maize domestication gene that establishes developmental boundaries and specifies meristem fates despite not being expressed within them. TSH4 accomplishes this by using a double-negative feedback loop that targets and represses the very same microRNAs that negatively regulate it. TSH4 functions redundantly with a pair of homologs to positively regulate a suite of domestication loci while specifying the meristem that doubled seed yield in modern maize. TSH4 has a critical role in yield gain and helped generate ideal crop plant architecture, thus explaining why it was a major domestication target.

Since wild teosinte is not suitable for agriculture, numerous changes in plant architecture were required to transform it into the maize crop we use today. In many grasses, a common suite of traits that comprise the well-characterized 'domestication syndrome' was selected during this transformation¹. These include a lack of seed shattering, a reduction in vegetative lateral branching (tillering) and a reduction in leafy floral organs. Some of these floral traits, however, conflict with what is desired during the vegetative phase, and thus it is critical that domestication genes have defined phase-specific functions. For example, during the vegetative phases of many crops, leaf growth predominates while the associated axillary meristems are repressed. During the floral phase, the reverse is often true where leaves are repressed and reproductive axillary meristems derepressed to enhance yield. One such axillary meristem is the spikelet pair meristem (SPM) that branches to form two spikelets, thus allowing maize to double its seed yield compared to its single spikelet-producing teosinte ancestor². While many domestication loci have been identified, the mechanisms by which they work and how they are able to have distinct functions during different growth phases remain mysterious. In addition, the identification of new domestication loci can be hampered by epistasis, in which the effects of one gene are dependent on the presence or absence of another³. This is especially true in maize where an epistatic network of several different gain-of-function mutations has been shown to be critical for domesticated plant architecture4.

The reduction in lateral branching in maize compared to teosinte was accomplished by selection for a dominant allele of the transcription factor TEOSINTE BRANCHED1 (TB1)5. TB1 in turn directly targets a host of other domestication genes⁴ including *grassy tillers1* (*gt1*), which controls lateral branch suppression⁶, teosinte glume architecture1 (tga1), which controls glume elaboration⁷, and tassels replace upper

State Key Laboratory of Maize Bio-breeding, National Maize Improvement Center, Frontiers Science Center for Molecular Design Breeding, China Agricultural University, Beijing, China. 2University of California, Berkeley/Plant Gene Expression Center, Albany, CA, USA. 3North Carolina State University, Raleigh, NC, USA. ⁴Brigham Young University, Provo, UT, USA. —e-mail: zbdong@cau.edu.cn; georgechuck@berkeley.edu

ears1 (tru1), which controls lateral branch growth and sex identity. Cloning of tb1 showed that it encodes a Teosinte branched1/Cincinnata/proliferating cell factor transcription factor that is overexpressed in maize due to the insertion of Hopscotch retrotransposon approximately 58 kb upstream of the promoter. Interestingly, all the TB1 targets mentioned above are either ectopically expressed in maize versus teosinte, overexpressed or, in the case of TGA1, have amino acid changes that lead to gain-of-function phenotypes. Thus, it appears that the domesticated architecture of maize largely resulted from a suite of different gain-of-function genes, all of which are directly targeted by TB1. This phenomenon may not be limited to maize, as orthologs of several of these same genes were breeding targets in other grasses including barley¹⁰ and wheat.

The formation of boundaries between adjoining cell populations possessing distinct identities is essential for differentiating the development of leaves from axillary meristems. For example, a unique boundary exists between the indeterminate cells of meristems and the determinate leaves initiated off their flanks¹². One mechanism for the establishment of these boundaries is through mutual negative regulation, a process that can effectively divide adjacent populations at cell-to-cell resolution as seen in several animal systems such as *Drosophila*¹³. In plants, this could be achieved through microRNA-mediated repression of target genes, thereby sequestering each other to adjacent, but opposing fields. For example, it has been shown that microRNAs often occupy distinct, although overlapping, domains compared to their targets within meristems¹⁴. Once two opposing fields are established, boundary-specific genes may be expressed at their borders, including lateral organ boundaries (LOB) transcription factors that occupy boundaries between meristem and leaves¹⁵. In maize, floral-specific LOB genes exist, such as ramosa2 (ra2) that is first expressed in the SPM to control meristem determinacy and identity16. Interestingly, many LOB genes are known to be regulated by auxin and have auxin response factor binding sites in their regulatory sequences¹⁷, indicating that phytohormones may also have roles in defining boundaries and distinguishing determinate versus indeterminate fates.

Here we identify the diverse mechanisms by which the maize SBP-box transcription factor tasselsheath4 (tsh4) establishes leaf versus meristem boundaries and vegetative versus floral meristem fates as part of a domestication gene network. Genome-wide mapping of domestication traits in maize/teosinte recombinant inbred populations uncovered tsh4 as a major locus responsible for multiple floral and vegetative domestication traits. We performed TSH4 chromatin immunoprecipitation followed by sequencing (ChIP-seq) and identified a suite of downstream genes that affect boundary formation, leaf repression and axillary meristem growth. Interestingly, these boundaries form through mutual negative regulation between the microRNAs that repress *tsh4* but are also negatively regulated by it. We show that *tsh4* and related paralogs work together to target several domestication loci, including those responsible for axillary meristem suppression such as tb1. These diverse mechanisms reveal how tsh4 was able to coordinate the broad range of critical floral and vegetative morphological changes demanded by early farmers during maize domestication.

Results

Genome-wide association analysis of domestication traits

Several traits associated with maize domestication and improvement were scored and quantitatively mapped in a previously described set of 866 maize–teosinte BC2S3 recombinant inbred lines (RILs) 18 , as well as a second pooled set of 1,257 maize–teosinte BC1S4 RILs called the teosinte nested association mapping (TeoNAM) population 19 . Quantitative trait loci (QTLs) associated with these traits mapped to a common interval containing tsh4 in both populations, identifying it as a strong candidate gene. These QTLs influence domestication traits

such as tiller number (TILN), percentage staminate spikelets (STAM), kernel weight (KW) or tassel branch number (TBN), a maize improvement trait. The QTLs STAM7.1 ($P = 2.44 \times 10^{-9}$), TBN7.2 ($P = 2.22 \times 10^{-5}$) and KW7.1 ($P = 1.19 \times 10^{-6}$) mapped to tsh4 by joint-linkage mapping in the TeoNAM population (Fig. 1a). Interestingly, the same STAM7.1 and TBN7.2 QTL were also detected in several of the single teosinte parent populations (single-pop QTL) for the BC1S4 lines (Fig. 1a). Moreover, another single-pop QTL, TILN7.1, exhibited a high logarithm of the odds (LOD) score of 21.29 and mapped to tsh4 in the BC2S3 population (Fig. 1a). Notably, tsh4 was the only gene in common for all four QTL intervals based on physical position (Fig. 1a). RIL populations were used to compare the phenotypic effects of the teosinte versus maize tsh4 alleles. This demonstrated that the maize tsh4 allele reduces TILN, STAM and TBN while increasing KW (Fig. 1b-e). Thus, selection for the maize tsh4 locus during domestication facilitated a reduction in vegetative lateral branching and helped specify lateral branch sex identity, which ultimately resulted in increased KW. After domestication, further selection on tsh4 may have resulted in reduced TBN, a desirable maize improvement trait. Given that tsh4 alone does not affect vegetative branching or lateral branch sex determination²⁰, a re-analysis of tsh4 gene function was undertaken.

tsh4 functions redundantly with ub2 and ub3

A previous analysis of tsh4 mutants revealed potential functional redundancy with its duplicated paralogs unbranched2 (ub2) and unbranched3 (ub3) with respect to vegetative development²¹, but the floral phenotype was unclear. To remedy this, the inflorescences of two different ub2/ub3/tsh4 triple mutant combinations were analyzed in the W22 and B73 backgrounds, with both showing identical phenotypes. In wild-type (WT) tassels and ears, several specialized axillary meristems are made, each producing unique reproductive structures²². In tassels, the main inflorescence meristem first initiates several tassel branch $meristems\,(BM), before\,producing\,ordered\,rows\,of\,SPM\,that\,initiate\,in$ the axils of rudimentary, suppressed bract leaves²³ (Fig. 1f,k). The SPM then widens transversely and branches to form two spikelet meristems (SM), each capable of initiating single spikelets that produce kernels in straight rows in ears (Fig. 1g,k). An analysis of triple mutant tassels showed that they were shorter and lacked BM compared to WT (Fig. 1f). Interestingly, subtending bract leaves were derepressed throughout both male and female triple mutant inflorescences (Fig. 1f-g), each subtending single spikelets instead of paired spikelets. In ears, the lack of paired spikelets manifests as disordered rows, something not seen in either tsh4 or ub2/ub3 mutants that maintain straight, ordered rows (Fig. 1g). In triple mutant tassels, single spikelets were often hidden in the axils of large derepressed bract leaves (Fig. 1h). Finally, triple mutants also overproduce tillers, phenotypes not seen in WT (Fig. 1i), tsh4 or ub2/ub3 doubles. The meristems at the tips of the derepressed tillers often have mixed sex identities instead of being strictly male, as observed in WT (Fig. 1j).

To determine the origin of the derepressed bract leaf and unpaired spikelet phenotypes, scanning electron microscopy (SEM) was performed. In triple mutant tassels, BM are not initiated, and all bract leaves are derepressed and grow before SPM formation (Fig. 11) compared to WT (Fig. 1k). Furthermore, the meristems that form in the axils of the derepressed bracts do not have SPM activity because they only initiate single spikelets (Fig. 11). To understand these phenotypes, we performed immunolocalization with the meristem identity and boundary marker RAMOSA2 (RA2). RA2 protein normally localizes as a ring at the base of, and throughout the SPM, the base of the SM (Fig. 1m), and is absent from lateral organs¹⁶. In triple mutants, however, RA2 is ectopically expressed in the derepressed bract leaves and downregulated in meristems (Fig. 1n,p), indicating that the SPM boundary and identity are altered. This derepression of lateral organs and loss of BM and SPMs results in greatly reduced yield in both the male and female triple mutants (Fig. 1f,g).

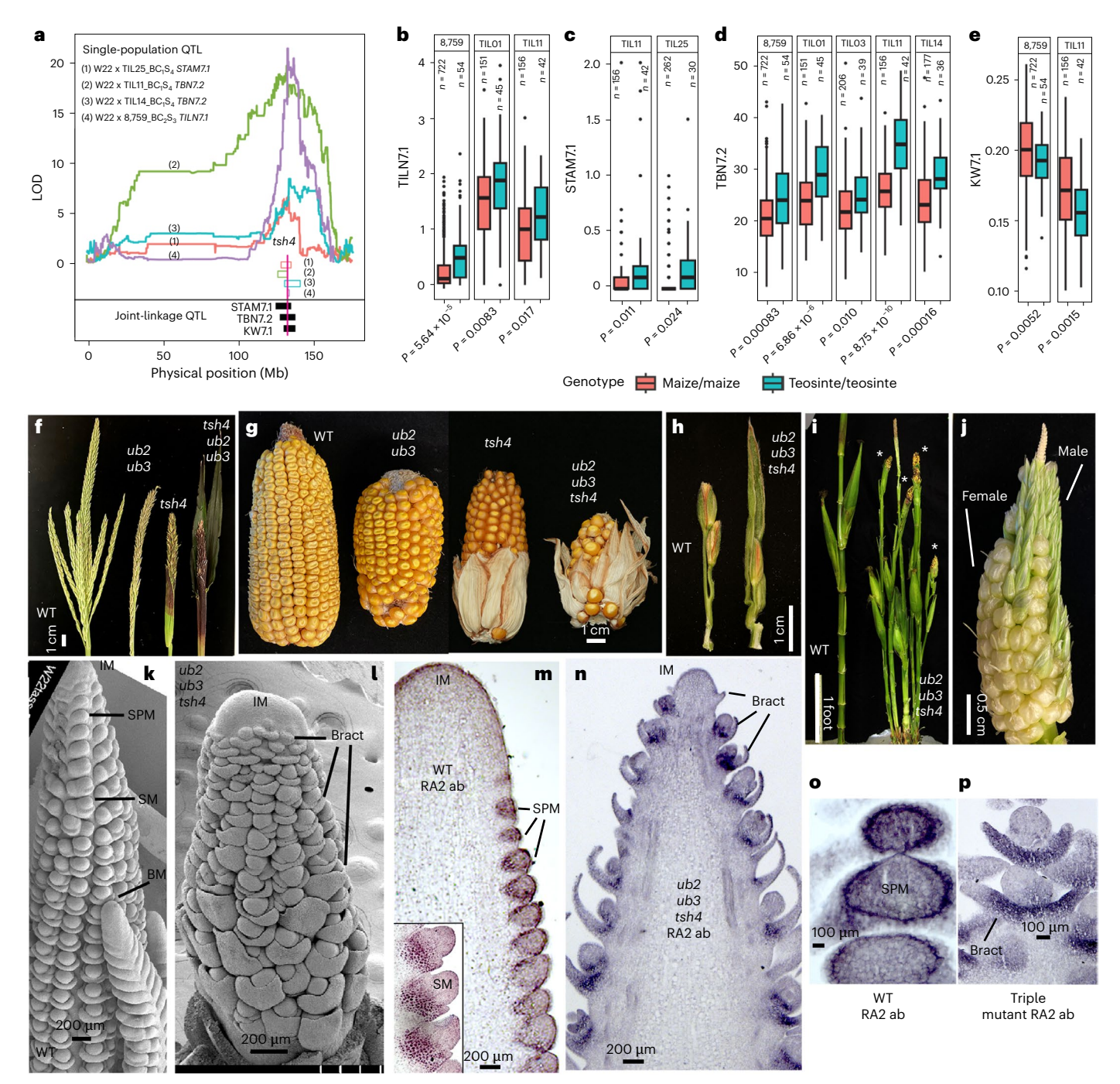


Fig. 1 | tsh4 affects domestication traits. a, Four domestication and improvement QTLs were mapped to the tsh4 gene in six different W22 maizeteosinte mapping populations. Single-population QTLs are displayed as significant LOD-colored curves on top, and multipopulation joint-linkage TeoNAM QTLs are displayed on the bottom. QTL support intervals are plotted as horizontal bars. The gene position of tsh4 is indicated by a vertical red line. b-e, Maize versus teosinte tsh4 allele effects with teosinte donor parents listed at the top: (b) TILN7.1, (c) STAM7.1, (d) TBN7.2 and (e) KW7.1. For box and whisker plots in Fig. 1b-e, the centerline indicates the median. The box extends from the 25th to 75th percentiles, and whiskers show minimum to maximum values. The lower and upper hinges correspond to the first and third quartiles. The upper whisker extends from the hinge to the largest value no further than 1.5× IQR from the hinge. The lower whisker extends from the hinge to the smallest value, at most 1.5× IQR of the hinge. A two-tailed t-test was used to determine P values. n = number of RILs. f, WT, ub2-mum1/ub3-mum1, tsh4-mum1 and tsh4-mum1/ub2-mum1/ub3-mum1 triple mutant tassels in the B73 background. The lowermost bract leaves were removed in tsh4, and the triple mutant to

reveal a lack of branches. g, WT, ub2-mum1/ub3-mum1, tsh4-mum1 and triple mutant ears. Bottom-most bract leaves were removed to reveal single kernels. h, Dissected tassel spikelet pair of WT (left), and single spikelet in the axil of the bract leaf of the triple mutant (right). i, WT B73 flowering plant compared to the triple mutant plant. Stars indicate tiller branch tips. **j**, Closeup of triple mutant tiller branch tip displaying mixed sex identity. k, SEM of WT tassel showing IM, initiating SPM, SM and BM. I, SEM of triple mutant tassel showing derepressed bract leaves and lack of BM or SPM. m, RA2 immunolocalization on WT showing expression in SPM. The inset shows expression at the base of the SM. n, RA2 immunolocalization on triple mutant showing ectopic expression at the base of derepressed bracts that form before the meristems. o, Sagittal view of RA2 immunolocalization on WT SPM showing a boundary formed by a ring of expression at the base. **p**, Sagittal view of RA2 immunolocalization on triple mutant meristem showing ectopic expression in bracts accompanied by loss of meristem expression. Scale bars: **f-h**, 1 cm; **l**, 1 foot; **j**, 0.5 cm; **k-n**, 200 μm; **o** and p, 100 µm. IM, inflorescence meristem; IQR, interquartile range.

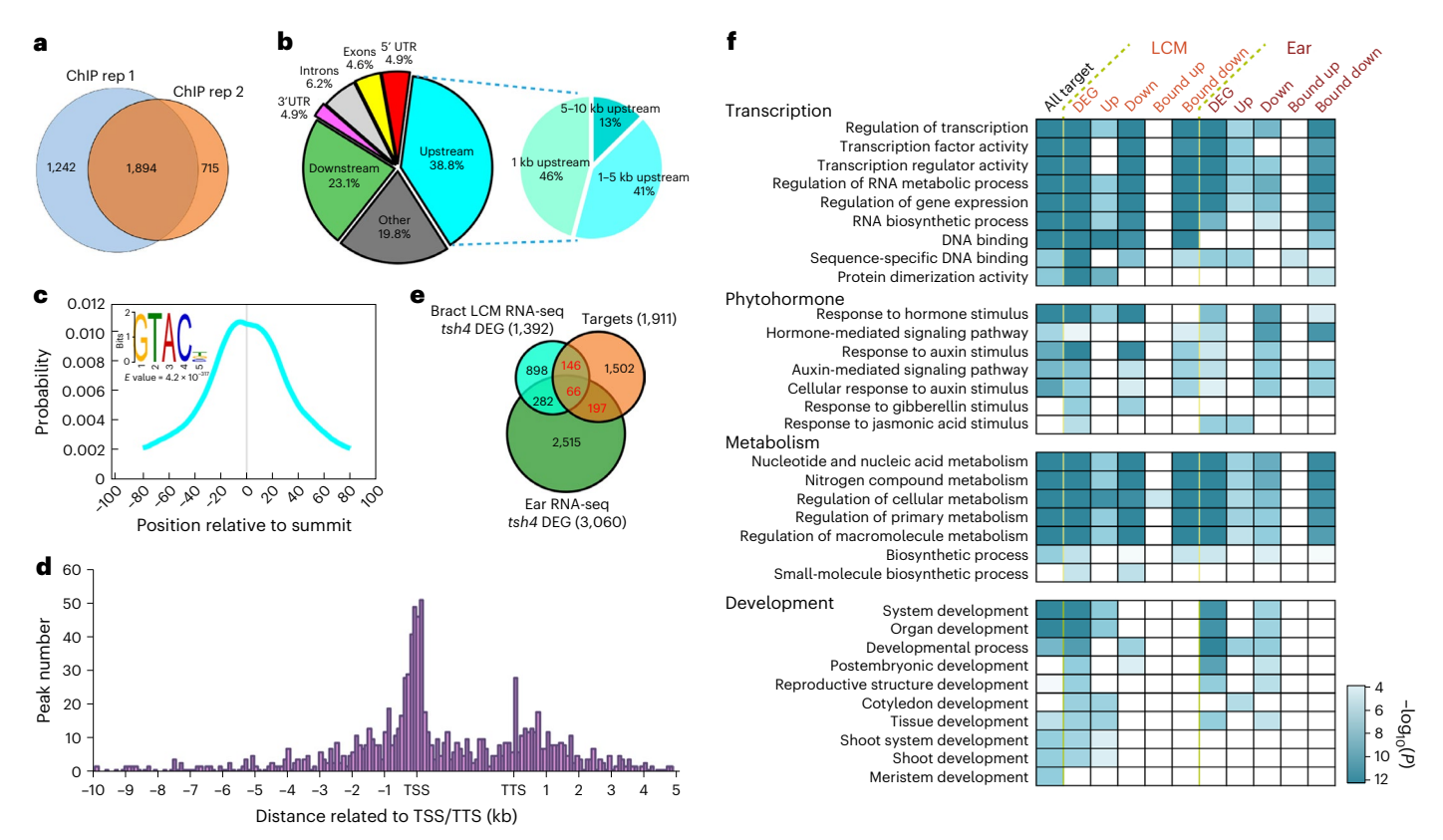


Fig. 2| **Identifying TSH4 direct targets using ChIP-seq. a**, Overlap between two TSH4 ChIP-seq replicates using young ear chromatin relative to IgG controls. **b**, Genome-wide distribution of TSH4-binding peaks showing that the majority of peaks (over 80%) are located in genic regions. **c**, Enrichment of GTAC SBP-binding motifs within the TSH4-binding peaks and location relative to peak summits.

d, Distribution of TSH4-binding peaks relative to gene models. TSS, transcription start site; TTS, transcription termination site. **e**, Overlap of all TSH4 targets by ChIP–seq with *tsh4* DEGs by LCM RNA-seq of bracts, and bulk tissue RNA-seq of young ears. **f**, Functional categories of all TSH4 ChIP–seq targets and *tsh4* DEGs identified in **e**.

TSH4 ChIP-seq

To identify the genes responsible for the lack of BM and SPM and the loss of the SPM/bract boundary, we performed ChIP-seq on 3-5 mm B73 ear primordia using a TSH4 antibody²⁰. Using previously described protocols⁴, two biological replicates were sequenced, identifying 2,609 and 3,136 high-confidence peaks, respectively (Fig. 2a), compared to immunoglobulin G (IgG)-negative controls. In total, 1.894 of these peaks were common to both libraries, the vast majority (80.2%) mapping to genic regions (Fig. 2b). A MEME analysis identified a GTAC motif located at peak summits (Fig. 2c) similar to the core consensus-binding motif of SBP-box transcription factors²⁴. We correlated reproducible peaks with potential target genes by requiring them to map within 10 kb upstream and 5 kb downstream. This identified 1,911 possible target genes, most of which were bound by TSH4 within 1 kb of the transcription starts (Fig. 2d). To determine which of these were transcriptionally modulated in tsh4, we correlated the peaks with tsh4 differentially expressed genes (DEGs) identified by RNA sequencing (RNA-seq) on young ears (Fig. 2e). Although 3,060 DEGs were found, only 263 of them were ChIP-seq targets. We reasoned that the number of target genes in meristematic young ears was reduced because TSH4 is not found in meristems²⁰, and thus only a fraction of this tissue expressed TSH4. To address this problem, we took advantage of an RNA-seq library derived from laser-capture microdissected (LCM) suppressed bract tissue where TSH4 is known to be expressed25. This library identified an additional 1,392 DEGs, of which 146 were additional ChIP-seq targets. Taken together, 409 tsh4 DEGs were found to be bound by TSH4 using ChIP-seq, comprising a pool of high-confidence direct target genes. Gene ontology (GO) term analysis of the combined DEGs revealed enrichment in genes

that function in transcription, phytohormone response and signaling, metabolism and development (Fig. 2f).

TSH4 targets auxin response regulators

Since the triple mutant displays branching phenotypes also observed in auxin mutants²⁶, auxin targets were analyzed in greater detail. We identified members of the auxin/indole-3-acetic acid (Aux/IAA) response gene families as consistent direct targets of TSH4 (Fig. 3a). To confirm that these same genes were also targeted by UB2 and UB3, we took advantage of a previous DNA affinity purification sequencing (DAP-seq) dataset of putative TSH4, UB2 and UB3 targets²⁷ to identify peaks that may overlap with those from TSH4 ChIP-seq. While rare instances of overlap were found between all four datasets, such as those for ZMIAA14 (Fig. 3a), more often we found target genes that displayed clear ChIP-seq peaks, but inconsistent, or unclear DAP-seq peaks. This latter group includes the maize bif4 Aux/IAA gene that causes an unbranched inflorescence when mutated²⁸, as well as several other Aux/IAAs that have not been functionally characterized yet such as ZMIAA2, ZMIAA8 and ZMIAA14 (Fig. 3a). The TSH4 ChIP peaks at the bif4 locus were validated by additional independent ChIP-qPCR (Fig. 3b), and thus it is not clear why no DAP-seq peaks were found for this locus. Thus, we relied only on the TSH4 ChIP-seq data to find downstream targets but used the DAP-seq data if it overlapped and agreed with the ChIP-seq data (Supplementary Note). We confirmed that these Aux/IAA genes are in fact downregulated in tsh4 single, ub2/ub3 double, as well as triple mutants (Fig. 3c), indicating that they are activated by all three SBP proteins. Because Aux/IAA genes are known to function as repressors that negatively regulate auxin response²⁹, these results suggest that SBPs may restrict the growth of floral bracts

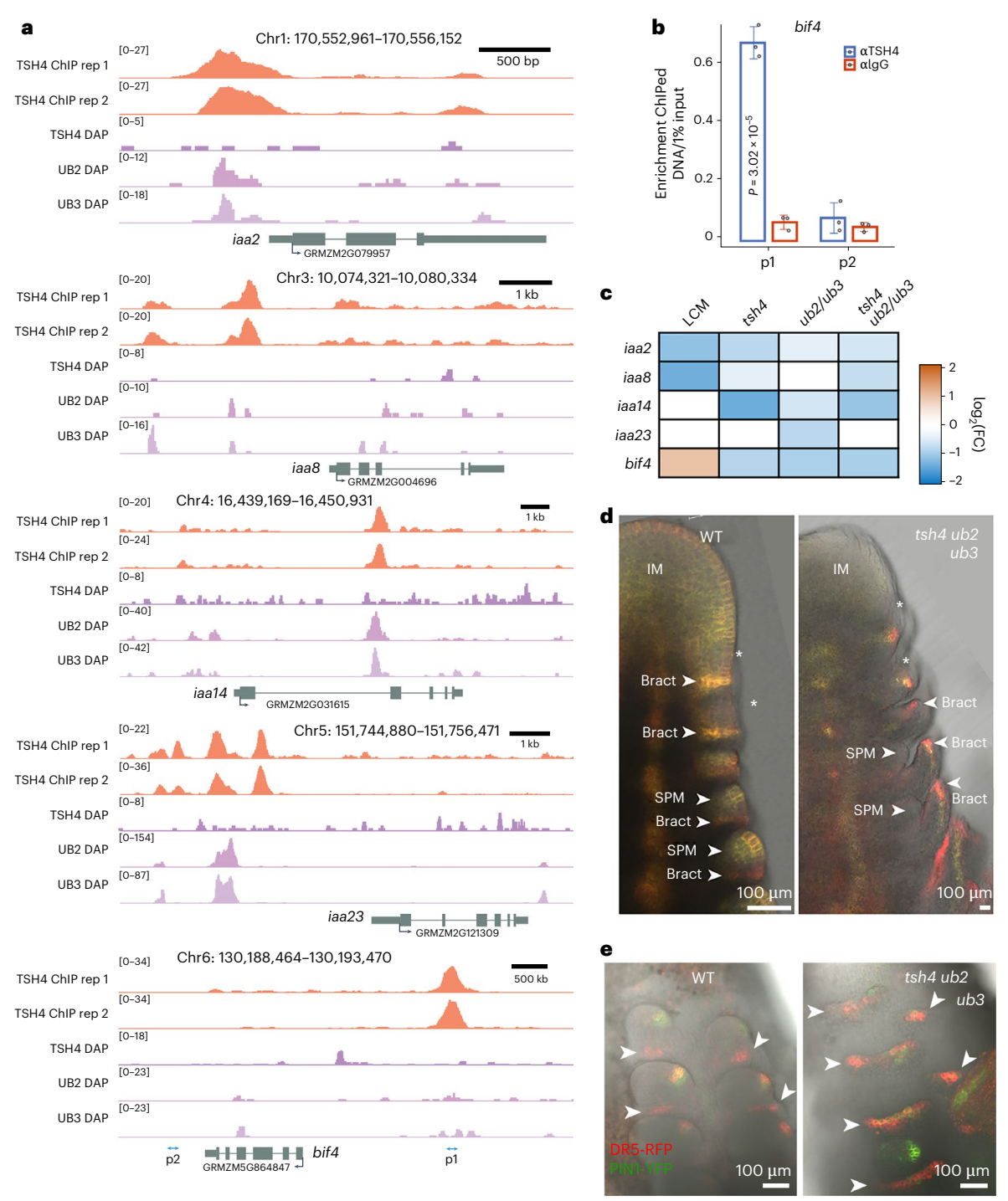


Fig. 3 | **TSH4, UB2 and UB3 control auxin response. a**, TSH4-binding profiles near Aux/IAA genes from two TSH4 ChIP—seq replicates and TSH4, UB2 and UB3 DAP-seq peaks. **b**, Validation of TSH4 bif4 binding peaks using independent ChIP—qPCR (n=3 biological replicates). p1 amplification located at the ChIP—seq peak is significantly enriched in WT chromatin (blue bars) compared to the p2 site versus IgG controls (orange bars). Error bars are presented as means \pm s.d. P value calculated from two-tailed t-test. **c**, Expression of Aux/IAA target genes in

tsh4 bracts, ears of tsh4 and ub2/ub3 mutants and triple mutants. The gradient color scale indicates the log value of expression fold change (log_2(FC)). \mathbf{d} , Auxin response (DrSrev::mRFPer) and transport (PZmPIN1a::ZmPIN1a::FP) in the suppressed bracts and SPMs of WT (left) compared to the triple mutant (right) ears. Asterisks indicate SPM anlagen. Scale bar, 10 μ m. \mathbf{e} , Sagittal view of auxin response and transport in WT (left) and the triple mutant (right) SPM with bracts (arrowheads). Scale bar, 100 μ m. Chr, chromosome.

in WT by repressing their ability to sense auxin. If so, enhanced auxin response should be expected in the growing, derepressed bracts of triple mutants. To test this, we introgressed triple mutants into the *pZmPIN1a::*

in early repressed bracts (Fig. 3d). Later, this fluorescence was lost as the bracts were suppressed, but observed throughout the SPM instead (Fig. 3d) as well as off its flanks (Fig. 3e). In comparison, triple mutants exhibited enhanced high fluorescence at the tips of the derepressed bracts with very little in the SPM (Fig. 3d,e). Taken together, these data indicate that in the triple mutant, most of the auxin transport and

response occurs in derepressed bracts at the expense of the associated axillary meristems.

TSH4 targets its own negative regulating microRNAs

Because the boundary marker RA2 was misexpressed in triple mutants (Fig. 1n,p), we sought to analyze other potential target genes that may function as boundary determinants, including microRNAs31. In total, 35 of 154 known maize microRNA genes are bound by TSH4, far more than would be expected by chance (Fig. 4a). To determine which of these microRNAs are modulated by TSH4, microRNA sequencing was performed on tsh4, ub2/ub3 double and triple mutant ears (Fig. 4b). Nine of them were upregulated, including MIR156 and MIR529, both of which are known to cleave tsh4 mRNA²⁰. Analysis of MIR529 and MIR156 expression via microRNA-qPCR confirmed that both are overexpressed in tsh4 single mutants, ub2/ub3 double and the triple mutants (Fig. 4c), indicating that they are repressed by TSH4 and UB2/UB3. The locations of the TSH4 ChIP-seq peaks in the MIR156 and MIR529 promoters overlapped very well with UB2/UB3 DAP-seq peaks and were validated by additional ChIP-qPCR (Fig. 4d). Taken together, these data indicate that these microRNA genes are bound and repressed by all three SBP proteins.

The fact that TSH4 binds to, and represses, the same microR-NAs that negatively regulate it raises the intriguing possibility of a double-negative feedback loop³² acting between them. We hypothesized that this could establish a tight boundary between SPMs and bracts and clarify why this boundary is absent in triple mutants. To determine if this mechanism was feasible, we examined the timing and spatial expression of TSH4 and MIR529 using simultaneous TSH4 immunolocalization and microRNA in situ hybridization. TSH4 protein is not found in any meristem and is expressed at high levels in bract primordia and stems²⁰ (Fig. 4e). Conversely, MIR529 is expressed in meristems but not bract primordia (Fig. 4f). In triple mutants, MIR529 is ectopically expressed in both bracts and SPMs (Supplementary Fig. 1a), while the sense control showed no expression (Fig. 4f, inset). A simultaneous MIR529 in situ hybridization and TSH4 immunolocalization revealed that the microRNA is expressed in the IM first but later overlaps with TSH4 in the bract anlagen (Fig. 4g, top-right inset). At this point, TSH4 can be observed in the nuclei, while MIR529 can also be seen in the cytoplasm of the same cells (Fig. 4g, top-right inset). Later, a high degree of expression overlap still occurs in the growing bract primordium (Fig. 4g, bottom-right inset), but less overlap is observed in the initiating SPM anlagen as TSH4 begins to be cleared from the nuclei. Once the SPM is established and bract suppression occurs, they no longer overlap, with MIR529 localizing to the cytoplasm of the SPM while TSH4 is relegated to the nuclei of a thin strip of cells subtending the SPM in the remnant bract (Fig. 4g, bottom-right inset). These observations are consistent with TSH4 and MIR529 gradually establishing exclusive expression domains in the developing inflorescence through mutual negative regulation. This boundary only begins to stabilize once the switch in fates occurs and the two adjacent fields between the meristem and lateral organ are cemented.

TSH4 targets domestication loci

Because the association analysis indicated that *tsh4* controls domestication traits (Fig. 1a–e), we investigated whether TSH4 targets known maize domestication genes. We confirmed that *tb1* is a TSH4 target with ChIP–seq peaks located adjacent to a *Hopscotch* transposon insertion located 58 kb upstream of the *tb1* promoter (Fig. 5a), a known domestication site important for tiller repression³³. These ChIP–seq peaks also overlap with putative UB2- and UB3-binding sites identified by DAP-seq (Fig. 5a). Immunolocalization of TSH4, TB1 and UB2/UB3 in adjacent sections of young maize and teosinte tiller bud primordia indicates that all three proteins overlap (Supplementary Fig. 1b), consistent with these SBPs having a role in tiller repression.

The lateral branches of triple mutants are very long and have mixed sex identities instead of being only female (Fig. 1i), a phenotype known to be controlled by the *tru1* domestication gene⁸. We found that *tru1* is another TSH4 ChIP target with peaks located in the first intron near UB2 and UB3 DAP-seq peaks (Fig. 5a). Because TSH4-binding sites are typically located in promoters rather than introns (Fig. 2b), we performed additional ChIP-qPCR to validate this result and found that TSH4 binding is in fact enriched in the intron (Fig. 5b). A third domestication gene that controls glume hardness, tga1, is another TSH4 direct target that has overlapping UB2 and UB3 DAP-seq peaks (Fig. 5a), although we observed no clear glume defects in triple mutants. To determine if tb1, tru1 and tga1 are activated or repressed by the SBP proteins, we performed RT-qPCR on different WT tissues and two different triple mutant combinations. Both tb1 and tru1 were confirmed to be significantly downregulated in triple mutant shoots, while tga1 was downregulated in triple mutant ears, indicating that the SBP genes function to activate these domestication genes (Fig. 5c).

Differential activity of the maize versus teosinte tsh4 alleles

We investigated whether there were any activity differences between the maize versus teosinte tsh4 alleles and whether this correlated with differential expression of domestication genes. Interestingly, the maize tsh4 allele was expressed at higher levels than the teosinte allele in tassel and ear tissue (Fig. 5d). We used maize near-isogenic lines (NILs) derived from the W22-teosinte BC2S3 population to assay whether the teosinte versus maize tsh4 alleles were more efficient at activating expression of the domestication genes within a maize background. Indeed, we found that tb1 and tga1 were more highly expressed by the domesticated tsh4 W22 maize allele compared to the teosinte allele in the same background (Fig. 5e). In contrast, the ub2 and ub3 genes were not differentially expressed by either tsh4 allele as expected (Fig. 5e). Thus, it appears that a high-expressing domesticated tsh4 allele may have a role in facilitating the tb1 or tga1 gain-of-function phenotypes in maize compared to teosinte.

Diversity scans

Because the association analysis indicated tsh4 was a domestication and improvement target, we analyzed its nucleotide conservation in maize, maize landraces and teosinte. We observed that diversity decreased dramatically within the genic region of tsh4 in domesticated modern maize and landraces compared to teosinte (Fig. 5f). Taiiima's D values were significantly negative across the entire maize tsh4 locus compared to the teosinte, indicating that the domesticated maize allele was under stronger positive selection (Fig. 5f,g). A relative comparison of the coding versus noncoding regions of several sequenced maize and teosinte tsh4 genes pointed to the first intron as being responsible for the bulk of the differences (Fig. 5g and Supplementary Fig. 1c). To examine the degree of nucleotide divergence in this region, the entire *tsh4* genes from 15 different teosinte accessions were amplified, sequenced and compared to those of the entire maize nested association mapping (NAM) founder population that represents the range of diversity found in modern maize³⁴ (Supplementary Fig. 2). This analysis uncovered several amino acid changes and numerous small deletion and insertion polymorphisms centered in the first intron (Fig. 5g) and one 60 bp deletion present only in maize (Supplementary Fig. 2). Because transient expression assays comparing the activity of the maize versus teosinte first introns gave mixed results, the functional significance of this region is unclear. Despite this, the fact that a single haplotype exists in modern maize, coupled with the association analysis and the identification of target genes, supports tsh4 as a new domestication locus that sits atop of a large gene network (Fig. 5h).

Discussion

Like many other grass crops, maize leaves are elaborated during the vegetative phase while their associated axillary buds are repressed.

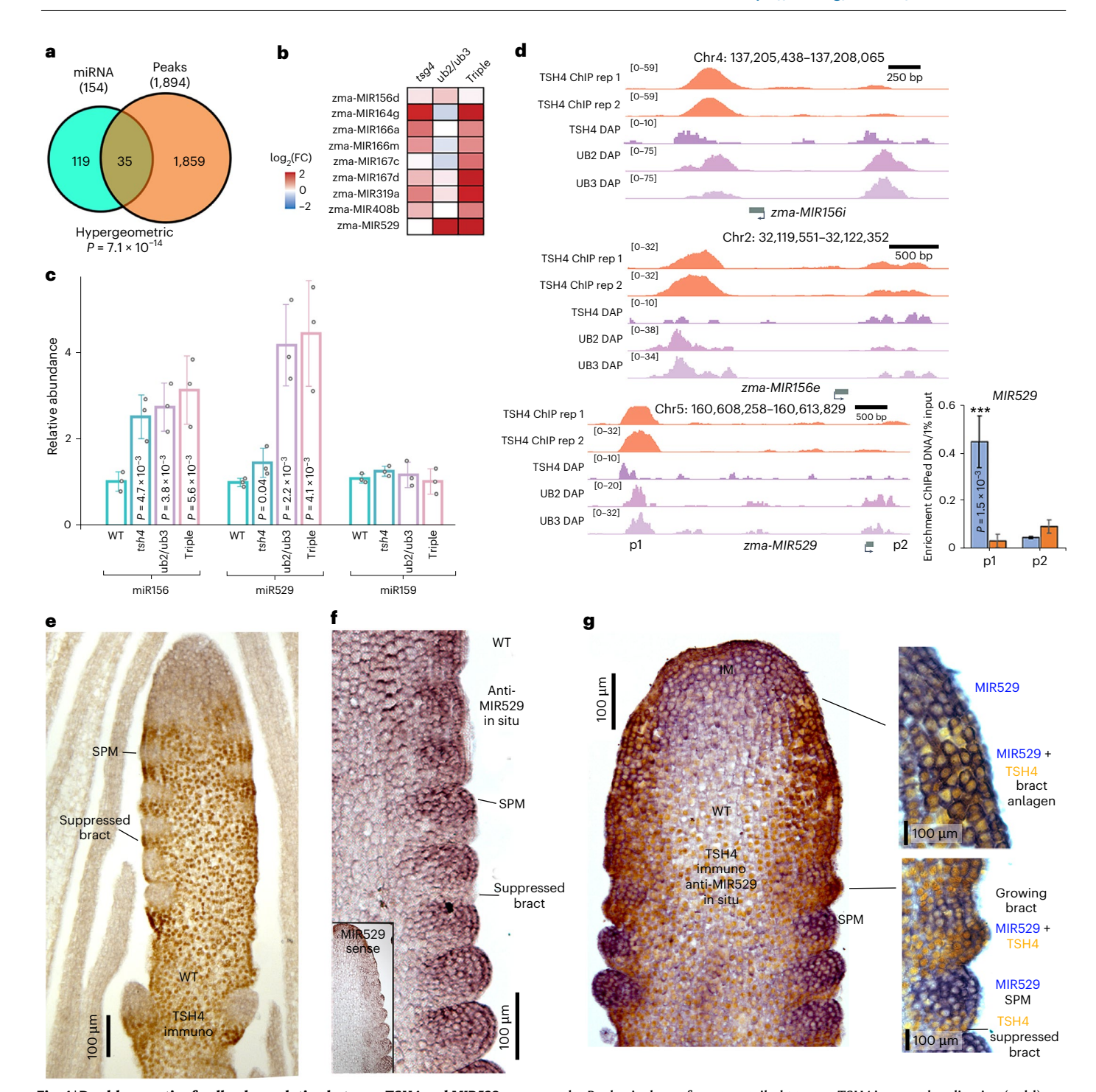


Fig. 4 | **Double-negative feedback regulation between TSH4 and** *MIR529.* **a**, Overlap between miRNA loci and TSH4-binding peaks. Significance confirmed by two-sided hypergeometric test. **b**, MicroRNA sequencing identified nine microRNAs that are upregulated in *tsh4*, double and triple mutants. **c**, RT-qPCR evaluation of mature miR156 and miR529 expression showing upregulation in *sbp* mutants. miR159, a nontarget, showed no difference. **d**, Examples of TSH4-binding profiles near representative miRNA genes, with two TSH4 ChIP-seq replicates as well as UB2 UB3 and TSH4 DAP-seq peaks. The inset shows qPCR validation of MIR529 peaks using primers located at the peak (p1) and downstream (p2). For **c** and **d**, error bars are presented as means ± s.d (n = 3), and

the *P* value is shown from two-tailed *t*-test. **e**, TSH4 immunolocalization (gold) on young tassel showing protein in the stem, suppressed bract leaves, but missing in IM and SPM. **f**, Anti-MIR529 in situ hybridization on tassel showing expression in SPM, but not in bracts. Inset shows a sense control. **g**, Double labeling of tassel primordium with MIR529 antisense microRNA in situ (blue) and TSH4 antibody (gold). Enlarged insets of the same primordium on the right taken under differential interference contrast (DIC) filters, demonstrating overlap in the bract anlagen (top right), but loss of overlap and complementary expression at the bract suppression stage (bottom right). Scale bars, $100 \ \mu m \ (e-g)$. ***Significant *P* value < 0.05.

After the switch to reproductive growth, however, leaves are repressed while the axillary floral buds are elaborated. This growth habit is the result of nearly 10,000 years of selection because the progenitor of

maize originally had derepressed axillary buds during the vegetative phase and fewer reproductive axillary buds during the floral phase. Given the critical roles of floral structures in yield gain, it is

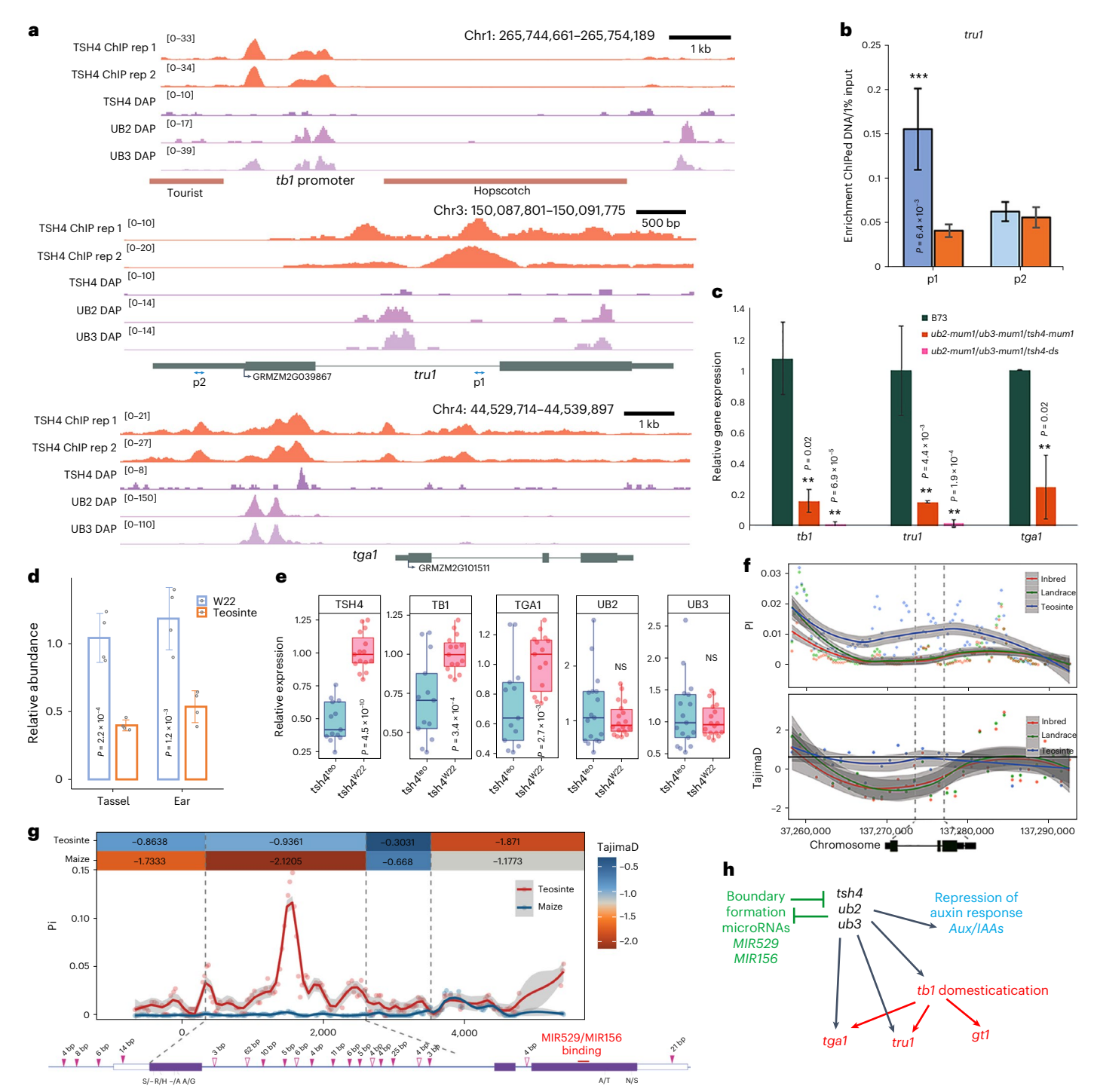


Fig. 5 | **TSH4** targets domestication loci. a, Location of SBP-binding peaks 58 kb upstream of the tb1 promoter flanking the Hopscotch retrotransposon insertion responsible for domestication, tru1 intron and tga1 promoter. **b**, Independent ChIP-qPCR validation showing enrichment of TSH4-binding peaks in tru1 intron (p1) compared to promoter (p2). *** $P = 6.4 \times 10^{-3}$. **c**, RT-qPCR analysis of domestication gene expression in 3-week-old B73 and triple mutant shoots (tb1 and tru1) and silking ears (tga1). **P = 0.02, ** $P = 6.9 \times 10^{-5}$, ** $P = 4.4 \times 10^{-3}$, ** $P = 1.9 \times 10^{-4}$ and **P = 0.02. **d**, RT-qPCR comparison of maize tsh4 versus teosinte tsh4 expression levels in tassels and ears. **b-d**, Error bars are presented as means \pm s.d. (n = 3 for **b** and **c**; n = 4 for **d**; and P values were calculated using a two-tailed t-test). **e**, RT-qPCR on ear tissue from maize/teosinte NILs demonstrating upregulation of tsh4, tb1 and tga1 in lines with the tsh4 maize alleles (pink) compared to sibs containing the teosinte alleles (blue; $n \ge 15$). The centerline indicates the median, and the box extends from the 25th to 75th percentiles. The upper whisker extends from the hinge to the largest value no

further than 1.5× IQR from the hinge, and the lower whisker extends from the hinge to the smallest value at most 1.5× IQR of the hinge. *P* values were calculated using a two-tailed *t*-test. NS, not significantly different. **f**, Nucleotide diversity (PI) (top) and Tajima's *D*-test (bottom) for the region surrounding the *tsh4* locus for maize, maize landraces and teosinte. Vertical gray dashed lines indicate the *tsh4* transcript start and endpoints. Gray outlines denote 95% confidence intervals. **g**, Evaluation of nucleotide diversity (Pi) and Tajima's *D*-test (top, colored boxes) within the *tsh4* gene using sequence data from 15 teosinte lines (red) and 25 maize NAM population inbreds (blue). The first intron of *tsh4* shows the strongest signal of selection. Below is the *tsh4* gene model showing the positions of relevant polymorphisms. Solid arrowheads indicate that the maize allele is an insertion relative to teosinte, and the hollow arrowheads indicate that the maize allele is a deletion; amino acid changes are labeled below. Gray outlines denote 95% confidence intervals. **h**, Model for *tsh4* function incorporating microRNAs, auxin response and domestication.

not surprising that early farmers selected plants with enhanced floral branching. We show how selection for *tsh4* could engender ideal plant architecture during vegetative growth by helping to repress vegetative axillary buds, while also improving yield during the floral phase by helping to initiate and pattern the reproductive buds. This architecture was achieved through the selection of a high-expressing *tsh4* allele that is more efficient in activating the expression of domestication genes (Fig. 5e) and functions to establish developmental boundaries through microRNA-mediated double-negative feedback loops.

TSH4 targets and represses two microRNA genes, MIR156 and MIR529, which in turn cleave *tsh4* transcripts. This mechanism is reminiscent of microRNA-mediated double-negative feedback autoregulation³⁵, leading to a cell fate switch between bract leaf versus SPM identity. Using simultaneous microRNA in situ hybridization and TSH4 immunolocalization, we were able to correlate the timing and location of this switch with developmental outcomes. Although both MIR529 and TSH4 proteins overlap in a common SPM/bract anlagen, their expression becomes mutually exclusive when SPM fates are established and bract growth is repressed (Fig. 4g, bottom inset), indicating that the switch in cell fates is complete. Interestingly, boundary genes such as RA2 begin to be expressed in developing SPMs (Fig. 1m,o) at this stage. Thus, it is likely that the establishment of the meristem/bract boundary is cemented at this point, and subsequent meristem-specific RA2 localization allows SPM identity to be acquired 16. In the absence of this boundary, RA2 localizes to the derepressed bract of the triple mutant (Fig. 1n,p), and SPM branching activity is lost. Because of this, we propose that in triple mutants, the SPMs lose their identities, becoming more determinant and making only single spikelets.

Interestingly, neither TSH4 (ref. 20) nor UB2 and UB3 (ref. 21) are expressed in BMs or SPMs, so the loss of both meristems in triple mutants is surprising. We hypothesized this results from derepressed bract leaves in triple mutants capturing hormonal resources normally used for branching and initiation events, thereby creating low auxin zones near axillary meristems that are commonly observed in other plants observed clear fluorescence signals for auxin transport and response throughout the WT SPM (Fig. 3d, left). In contrast, in triple mutants, high levels of fluorescence were seen in the derepressed bract leaves (Fig. 3d, right) but very low levels in the SPM, consistent with an auxin deficit in the meristem cells. Because auxin is critical for meristem branching and initiation in maize inflorescences, this deficit may also explain why the triple mutant SPMs do not branch and form two spikelets, or why BMs do not initiate.

In WT-suppressed bracts, our ChIP results indicate that a low auxin environment may result from the presence of TSH4, which binds and activates several *Aux/IAA* genes (Fig. 3a). Aux/IAA proteins function as repressors that bind the promoters of auxin-responsive genes and prevent their transcription³⁷. Thus, the strong expression of TSH4 in the primordial bracts, normally the site of local auxin maxima (Fig. 3d, left), may activate Aux/IAAs to block lateral organ development by preventing cells from responding to the hormone. The associated SPM, however, does not express TSH4 and is free to respond to auxin and ultimately branch to make two spikelets.

We show that *tsh4* promotes the domestication syndrome during the vegetative phase of plant development by repressing tillering but then promotes reproductive branching by repressing bract growth. The fact that the domesticated *tsh4* allele influences multiple agronomic traits during two different phases of development may explain why it was a major target of selection. We propose that *tsh4* should be considered a new domestication gene in light of the following lines of evidence: (1) QTL mapping using multiple maize/teosinte populations uncovered *tsh4* as a key locus controlling several domestication traits (Fig. 1a–e); (2) nucleotide diversity analysis confirmed that *tsh4* is under strong selection (Fig. 5f,g), with few haplotypes present in modern maize but multiple haplotypes present in wild teosinte (Supplementary Fig. 2);

and (3) genetic and molecular analysis showed that TSH4, together with UB2 and UB3, binds and activates several known domestication genes (Fig. 5a) and affects domestication phenotypes when mutated (Fig. 1f–j). Given the importance of these *SBP* genes during domestication, it is curious that they were not identified by previous studies. Given their positions at the top of the domestication hierarchy (Fig. 5h), it is possible that epistasis and functional redundancy may have concealed their presence. Because of this, implementing ChIP–seq together with higher-order genetic analysis, QTL mapping and nucleotide diversity analysis were all required to uncover a domestication role for *tsh4*. There is no doubt that many more domestication loci will be uncovered in maize by taking advantage of these diverse genetic resources, and only then will we gain a clearer understanding of how ancient farmers were able to transform a simple weed into the major crop plant we depend on today.

Online content

Any methods, additional references, Nature Portfolio reporting summaries, source data, extended data, supplementary information, acknowledgements, peer review information; details of author contributions and competing interests; and statements of data and code availability are available at https://doi.org/10.1038/s41588-024-01943-z.

References

- Harlan, J. R., de Wet, J. M. J. & Price, E. G. Comparative evolution of cereals. Evolution 27, 311–325 (1973).
- Stitzer, M. C. & Ross-Ibarra, J. Maize domestication and gene interaction. New Phytol. 220, 395–408 (2018).
- Doust, A. N. et al. Beyond the single gene: how epistasis and gene-by-environment effects influence crop domestication. Proc. Natl Acad. Sci. USA 111, 6178–6183 (2014).
- Dong, Z. et al. The regulatory landscape of a core maize domestication module controlling bud dormancy and growth repression. *Nat. Commun.* 10, 3810 (2019).
- Doebley, J., Stec, A. & Hubbard, L. The evolution of apical dominance in maize. Nature 386, 485–488 (1997).
- Whipple, C. J. et al. grassy tillers1 promotes apical dominance in maize and responds to shade signals in the grasses. Proc. Natl Acad. Sci. USA 108, E506–E512 (2011).
- Wang, H. et al. The origin of the naked grains of maize. Nature 436, 714–719 (2005).
- Dong, Z. et al. Ideal crop plant architecture is mediated by tassels replace upper ears1, a BTB/POZ ankyrin repeat gene directly targeted by TEOSINTE BRANCHED1. Proc. Natl Acad. Sci. USA 114, E8656–E8664 (2017).
- Studer, A., Zhao, Q., Ross-Ibarra, J. & Doebley, J. Identification of a functional transposon insertion in the maize domestication gene tb1. Nat. Genet. 43, 1160–1163 (2011).
- Ramsay, L. et al. INTERMEDIUM-C, a modifier of lateral spikelet fertility in barley, is an ortholog of the maize domestication gene TEOSINTE BRANCHED 1. Nat. Genet. 43, 169–172 (2011).
- Dixon, L. E. et al. TEOSINTE BRANCHED1 regulates inflorescence architecture and development in bread wheat (*Triticum aestivum*). Plant Cell 30, 563–581 (2018).
- Aida, M., Ishida, T., Fukaki, H., Fujisawa, H. & Tasaka, M. Genes involved in organ separation in *Arabidopsis*: an analysis of the cup-shaped cotyledon mutant. *Plant Cell* 9, 841–857 (1997).
- Kraut, R. & Levine, M. Mutually repressive interactions between the gap genes giant and Krüppel define middle body regions of the Drosophila embryo. Development 111, 611–621 (1991).
- Nogueira, F. T. et al. Regulation of small RNA accumulation in the maize shoot apex. PLoS Genet. 5, e1000320 (2009).
- Rast, M. I. & Simon, R. The meristem-to-organ boundary: more than an extremity of anything. *Curr. Opin. Genet. Dev.* 18, 287–294 (2008).

- Bortiri, E. et al. ramosa2 encodes a LATERAL ORGAN BOUNDARY domain protein that determines the fate of stem cells in branch meristems of maize. Plant Cell 18, 574–585 (2006).
- Okushima, Y., Fukaki, H., Onoda, M., Theologis, A. & Tasaka, M. ARF7 and ARF19 regulate lateral root formation via direct activation of LBD/ASL genes in Arabidopsis. Plant Cell 19, 118–130 (2007).
- Shannon, L. M., Chen, Q. & Doebley, J. F. A BC2S3 maize-teosinte RIL population for QTL mapping. *Maize Genet. Coop. News Lett.* 93, (2019).
- Chen, Q. et al. TeoNAM: a nested association mapping population for domestication and agronomic trait analysis in maize. *Genetics* 213, 1065–1078 (2019).
- Chuck, G., Whipple, C., Jackson, D. & Hake, S. The maize SBP-box transcription factor encoded by tasselsheath4 regulates bract development and the establishment of meristem boundaries. *Development* 137, 1243–1250 (2010).
- Chuck, G. S., Brown, P. J., Meeley, R. & Hake, S. Maize SBP-box transcription factors unbranched2 and unbranched3 affect yield traits by regulating the rate of lateral primordia initiation. Proc. Natl Acad. Sci. USA 111, 18775–18780 (2014).
- 22. Bonnett, O. T. Developmental Morphology of the Vegetative and Floral Shoots of Maize (Univ. Illinois Agricultural Experiment Station, 1953).
- 23. Whipple, C. J. et al. A conserved mechanism of bract suppression in the grass family. *Plant Cell* **22**, 565–578 (2010).
- 24. Cardon, G. et al. Molecular characterisation of the *Arabidopsis SBP-box* genes. *Gene* **237**, 91–104 (1999).
- Xiao, Y. et al. Boundary domain genes were recruited to suppress bract growth and promote branching in maize. Sci. Adv. 8, eabm6835 (2022).
- McSteen, P. Hormonal regulation of branching in grasses. Plant Physiol. 149, 46–55 (2009).
- Ricci, W. A. et al. Widespread long-range cis-regulatory elements in the maize genome. Nat. Plants 5, 1237–1249 (2019).
- Galli, M. et al. Auxin signaling modules regulate maize inflorescence architecture. Proc. Natl Acad. Sci. USA 112, 13372–13377 (2015).

- Luo, J., Zhou, J.-J. & Zhang, J.-Z. Aux/IAA gene family in plants: molecular structure, regulation, and function. Int. J. Mol. Sci. 19, 259 (2018).
- 30. Gallavotti, A., Yang, Y., Schmidt, R. J. & Jackson, D. The relationship between auxin transport and maize branching. *Plant Physiol.* **147**, 1913–1923 (2008).
- 31. Yekta, S., Tabin, C. J. & Bartel, D. P. MicroRNAs in the Hox network: an apparent link to posterior prevalence. *Nat. Rev. Genet.* **9**, 789–796 (2008).
- 32. Zhang, H.-M. et al. Transcription factor and microRNA co-regulatory loops: important regulatory motifs in biological processes and diseases. *Brief. Bioinform.* **16**, 45–58 (2015).
- Clark, R. M., Wagler, T. N., Quijada, P. & Doebley, J. A distant upstream enhancer at the maize domestication gene tb1 has pleiotropic effects on plant and inflorescent architecture. Nat. Genet. 38, 594–597 (2006).
- 34. Yu, J., Holland, J. B., McMullen, M. D. & Buckler, E. S. Genetic design and statistical power of nested association mapping in maize. *Genetics* **178**, 539–551 (2008).
- Cai, S., Zhou, P. & Liu, Z. Functional characteristics of a double negative feedback loop mediated by microRNAs. *Cogn. Neurodyn.* 7, 417–429 (2013).
- Wang, Q., Kohlen, W., Rossmann, S., Vernoux, T. & Theres, K. Auxin depletion from the leaf axil conditions competence for axillary meristem formation in *Arabidopsis* and tomato. *Plant Cell* 26, 2068–2079 (2014).
- 37. Liscum, E. & Reed, J. W. Genetics of *Aux/IAA* and *ARF* action in plant growth and development. *Plant Mol. Biol.* **49**, 387–400 (2002).

Publisher's note Springer Nature remains neutral with regard to jurisdictional claims in published maps and institutional affiliations.

Springer Nature or its licensor (e.g. a society or other partner) holds exclusive rights to this article under a publishing agreement with the author(s) or other rightsholder(s); author self-archiving of the accepted manuscript version of this article is solely governed by the terms of such publishing agreement and applicable law.

 \circledcirc The Author(s), under exclusive licence to Springer Nature America, Inc. 2024

Methods

Plant materials and growth conditions

The *tsh4-mum1*, *ub2-mum1* and *ub3-mum1* mutant plants were genotyped using previously described primers^{20,21}. Those plants used for bulk ear RNA-seq and other expression assays were introgressed into the B73 background at least four times and then grown in the field. The *tsh4-DS*, *ub2-mum1*, *ub3-mum1* triple mutant in the W22 background was obtained via a similar method. The teosinte–maize NIL lines MR961 and MR588 originating from the W22-teosinte BC2S3 population¹⁸ were genotyped as having the teosinte *tsh4* allele and introgressed into the W22 background two more times to reduce background effects. The heterozygous lines were then selfed and genotyped again to generate NILs containing the homozygous teosinte or maize *tsh4* alleles, respectively. All lines are available upon request.

Genome-wide association analysis

The single-pop QTL population of 866 maize-teosinte BC₂S₃ RILs made by a cross between W22 and Zea mays ssp. parviglumis accession 8759 was scored for 16 traits and over 50,000 markers using genotyping-by-sequencing as previously described18. A second 1,257 maize-teosinte BC₁S₄ RIL population (TeoNAM) derived from five different crosses between W22 and teosinte was scored for 22 traits and over 51,544 SNPs as previously described¹⁹. For the BC2S3 population, two generations of backcrossing to the recurring maize parent were made, followed by three generations of selfing, while for the TeoNAM population, there was one generation of backcrossing followed by four generations of selfing. QTL mapping in each single population was carried out using a multiple QTL model in R/qtl³⁸. The joint-linkage mapping was performed using a stepwise linear regression fixed model, while for the single QTL population, Haley-Knott regression was used. More details of the two strategies can be found in ref. 19. To analyze QTL allele effects, we used the accession 8759, TIL01, TIL03, TIL11 and TIL14 RIL families (Z. mays ssp. parviglumis lowland teosinte), as well as the TIL25 family (Z. mays ssp. mexicana highland teosinte). The allele effects at the population level were examined using the SNP genotypes at the tsh4 gene. The RILs with consistent genotypes across SNPs were divided into homozygous maize and teosinte alleles to test the trait difference, and P values were obtained using Student's t-test by dividing genotypes into maize $(tsh4^{W22})$ and teosinte $(tsh4^{teo})$ based on markers within the tsh4 gene.

Immunolocalization

Ear and shoot tissue at various stages were embedded in Paraplast Plus (Sigma-Aldrich, P3683), and standard paraffin sections were dewaxed in Histoclear and rehydrated in ethanol-water gradient as described previously³⁹. The slides were then immersed in 10 mM sodium citrate buffer (pH 6.0) and boiled for 3 min as described previously. PBS (1×), 2 mg ml⁻¹powder milk and 0.1% Triton X-100 were used to prepare the blocking regent. A 1:400 dilution of TSH4, UB2/UB3 or TB1 antibody was added to the slides and incubated at 4 °C for overnight. After three washes in the blocking solution, a 1/1,000 dilution of an anti-rabbit alkaline phosphatase (AP)-conjugated secondary antibody (Invitrogen) was added and incubated at room temperature for 1 h. After washing three times as mentioned above, the slides were immersed in TNM buffer (100 mM Tris-HCl pH 9.5, 100 mM NaCl and 50 mM MgCl2) for 10 min before developing in developing solution (20 µl of 5-bromo-4-chloro-3-indolyl phosphate (BCIP)/nitro blue tetrazolium (NBT) in 1 ml of 1× TNM buffer). dried and mounted. For the double labeling in situ hybridization of MIR529 followed by the TSH4 immuno experiment, we synthesized an anti-MIR529 dual DIG-labeled locked nucleic acid oligo 5'-T(A)GAT(C)ATGCTG(G)CAGC(T)TC(A)-3' (Eurogentec) and followed the in situ hybridization protocol⁴⁰. After staining in the developing solution, the tissue was blocked and subjected to immunolocalization using the protocol described above but developed using horseradish peroxidase (HRP) secondary antibodies with the Vectastain ABC kit with yellow-colored substrate.

ChIP

Young ear primordia of 3–5 mm were carefully dissected, cross-linked for 10 min in 1% formaldehyde solution under vacuum and quenched by adding glycine to a final concentration of 0.1 M. About 1 g of tissue was used for each biological replication of the ChIP experiment. Nuclei extraction and ChIP using the TSH4 antibody were performed as described previously⁴. Normal goat anti-rabbit IgG was used as a negative control. To validate putative TSH4 targets, three replicates of similar ear tissue were used for ChIP–qPCR assays using gene-specific primer pairs (Supplementary Table 1) and Fast Evagreen qPCR mix. Relative enrichment was calculated using the $\Delta\Delta$ CT method, and significant differences were evaluated through a t-test between anti-TSH4 precipitated samples and IgG-negative controls.

ChIP-seq

The concentration of ChIP yields DNA from each replicate was quantitated by Qubit (Invitrogen Qubit 4). Approximately 2 ng was used for ChIP-seq library construction by the NEXTflex ChIP-Seq Kit (Bioo Scientific, NOVA-5143-01) according to the manufacturer's protocol. Thirteen PCR cycles were performed for library amplification. The ChIP-seq libraries were quality-checked by a bioanalyzer and sequenced at the Illumina HiSeq 4000 platform, generating 50 bp single-end reads. All clean reads were aligned to the maize genome (Zea mays.AGPv3.30) using Bowtie2, allowing one mismatch⁴¹, and the resulting uniquely mapped reads with map quality >20 were used for peak calling using MACS2 software (v.2.1.0; https://github.com/taoliu/MACS). Significant peaks (q < 0.05) relative to the IgG control samples were identified in each of the two biological replicates, and reproducible peaks were then identified if summits from each replicate were positioned within 300 bp of each other. The upstream 50 bp and downstream 50 bp around the reproducible peak summits were extracted and submitted for motifenrichment analysis using the MEME program (v.4.11.2). Putative TSH4 target genes were assigned if reproducible peaks were found in the range from 10 kb upstream to 5 kb downstream of the gene. The bigwig files generated by MACS2 were visualized using the Integrated Genomics Viewer (v.2.16.0).

Transcriptome analysis

Here, 3-6 mm ear tissue was dissected from B73, tsh4, ub2/ub3 and triple mutants, respectively, and immediately frozen in liquid nitrogen. Only the first ear from the top of each plant was collected, and approximately 20 ears were pooled for one biological replicate with three biological replicates collected per genotype. Total RNA was isolated using TRIzol Reagent (Invitrogen, 15596026) according to the manufacturer's instructions. Library construction was performed using ScriptSeq v2 RNA-Seq Library Kit (Epicenter, SSV21106) according to the manufacturer's instructions and then sequenced on a HiSeq 2500 sequencer (Illumina) for 150 single-end reads. Sequence data analysis was conducted as described previously⁴. All of the clean reads were trimmed by Trimmomatic v.0.36 and mapped to the maize B73 v3 genome using STAR aligner v.2.6.0a with default parameter settings⁴². Reads were tested for differential expression with edgeR using a false discovery rate significance threshold of 0.05. GO analysis was performed through agriGO (v2.0)⁴³, and the results were visualized using ggplot2 in R.

Gene expression quantification by RT-qPCR

Total RNA was isolated from various ear tissue samples harvested using TRIzol Reagent (Invitrogen, 15596026) according to the manufacturer's instructions. For quantitative RT–PCR (RT–qPCR) analysis, cDNA was synthesized from DNase I-treated total RNA as described previously 4 . Tenfold diluted cDNA was used as a template in a 20 μ l Fast Evagreen qPCR mix, and the s.d. was calculated among three biological replicates for each sample. ZmGAPDH was used as the internal reference to normalize the expression data. The primers used for qPCR are listed in Supplementary Table 1.

Visualization of PIN1-YFP DR5-RFP

The *pZmPIN1a::ZmPIN1a-YFP* and *DRSrev::mRFPer* transgenic maize lines³⁰ were crossed to *tsh4 ub2 ub3* triple mutants, and after subsequent backcrossing followed by sib crossing, homozygous triple mutants positive for yellow fluorescent protein (YFP) and red fluorescent protein (RFP) were selected for fluorescence imaging. WT siblings positive for YFP and RFP were used as the control. All the replicate images were taken under a consistent setting of the Leica TCS SP8 confocal microscope. YFP was imaged using 514 excitation and 520–575 emission, while RFP was imaged using 594 excitation and 625–655 emission.

miRNA sequencing and data analysis

Total RNA was isolated by the same method as used for the transcriptome analysis and RT-qPCR. Small RNA-seq libraries were generated using NEBNext Multiplex Small RNA Library Prep Set for Illumina (NEB, E7300L) according to the manufacturer's instructions. Briefly, 3' and 5' adaptors were ligated to 3' and 5' end of small RNA, respectively. The first-strand cDNA was synthesized after hybridization with a reverse transcription primer. The double-stranded cDNA library was generated through PCR enrichment. After purification and size selection, libraries with insertions between 18 bp and 40 bp were isolated. Library quality was assessed on the Agilent 5400 system, quantified by qPCR and then sequenced on Illumina platforms with the SE50 strategy by Novogene Bioinformatics Technology. At least 10 M reads were generated for each sequencing sample. After quality control and removing the low-quality sequences, the reads from total sRNAs (18-28 nt) were extracted and validated by mapping to the maize reference genome without mismatch by Bowtie2 (ref. 41). sRNA sequences were aligned to maize miRNAs according to the miRbase database (http://www.mirbase.org/) and normalized against the total count of 18 to 28 nucleotide reads, reported as reads per million. Differential expression of miRNA was calculated as described previously44.

miRNA quantification by qPCR

Real-time quantification of microRNAs was performed by deploying a stem-loop RT–PCR strategy. The six-nucleotide extension at the 3′ end of the stem-loop reverse transcription primer and the forward and reverse primers for specific miRNAs were designed according to the target miRNA sequence obtained from the maize miRbase database. Stem-loop pulsed reverse transcription and the subsequent real-time PCR were done following the protocol described in ref. 45. The primers used are listed in Supplementary Table 1.

Diversity scans

Nucleotide diversity (*pi*) and Tajima's *D* around *tsh4* in maize and teosinte were calculated by vcftools 0.1.15 with sliding windows (window size 1,000 bp and step size 300 bp), using the third-generation *Z. mays* haplotype map (HapMap 3) data were downloaded from https://www.panzea.org. Genomic DNA from 19 teosinte lines (Supplementary Table 1) was isolated and used as a template for *tsh4* PCR and sequence analysis. Eight pairs of primers covering the *tsh4* region from 3 kb upstream of the TSS to 1 kb downstream of the TTS were designed, and PCR amplification was performed using 2× Phanta Max Master Mix (Vazyme). PCR products were ligated into pTOPO-Blunt Simple Vector using a Zaro Background pTOPO-Blunt Simple Cloning Kit (Aidlab) and transformed into Trans5α Chemically Competent Cell (TransGen Biotech). PCR-positive colonies were sequenced and used for comparative DNA diversity analysis.

Statistics and reproducibility

Statistical analyses used in this study are described in the Methods. Data are presented as mean \pm s.d. P values and sample sizes of biological replicates (n) are indicated or described in the legends of Figs. 1 and 3–5. Significance analysis was performed by two-tailed Student's t-test

for pairwise comparisons. Results with a P value < 0.05 were considered statistically significant. Experiments regarding the SEM observation, protein immunolocalization and miRNA in situ were repeated at least three times using tissues from different individual plants.

Reporting summary

Further information on research design is available in the Nature Portfolio Reporting Summary linked to this article.

Data availability

All RNA-seq and ChIP-seq data generated in this study have been deposited in the National Center for Biotechnology Information Sequence Read Archive (accession code PRJNA517683). The link for the BC2S3 population can be found at http://datacommons.cyverse.org/browse/iplant/home/shared/panzea/genotypes/GBS/v23/teoW22_BC2S3_GBS_phased_genos_imputed_20110423.zip and https://figshare.com/s/0d3aa121f8393c9b4720 (ref. 46). The TeoNAM population link is located at http://datacommons.cyverse.org/browse/iplant/home/shared/panzea/genotypes/GBS/TeosinteNAM and https://doi.org/10.6084/m9.figshare.9820178, respectively. The Zea_mays. AGPv3.30 genome is available at the maize gene database (www.maizegdb.org). All other relevant data supporting the key findings of this study are available within the article, in the Supplementary Information files or are available from the corresponding authors upon reasonable request.

Code availability

No custom code was generated. All code used to analyze the sequence data is publicly available in the SAMtools section of GitHub (https://github.com/samtools/samtools).

References

- 38. Broman, K. W., Wu, H., Sen, Ś. & Churchill, G. A. R/qtl: QTL mapping in experimental crosses. *Bioinformatics* **19**, 889–890 (2003).
- 39. Tsuda, K. et al. *KNOTTED1* cofactors, *BLH12* and *BLH14*, regulate internode patterning and vein anastomosis in maize. *Plant Cell* **29**, 1105–1118 (2017).
- 40. Pena, J. T. G. et al. miRNA in situ hybridization in formaldehyde and EDC-fixed tissues. *Nat. Methods* **6**, 139–141 (2009).
- 41. Langmead, B. & Salzberg, S. L. Fast gapped-read alignment with Bowtie 2. *Nat. Methods* **9**. 357–359 (2012).
- 42. Dobin, A. et al. STAR: ultrafast universal RNA-seq aligner. *Bioinformatics* **29**, 15–21 (2013).
- 43. Tian, T. et al. agriGO v2. 0: a GO analysis toolkit for the agricultural community, 2017 update. *Nucleic Acids Res.* **45**, W122–W129 (2017).
- Li, L. et al. Widespread microRNA degradation elements in target mRNAs can assist the encoded proteins. *Genes Dev.* 35, 1595–1609 (2021).
- Varkonyi-Gasic, E., Wu, R., Wood, M., Walton, E. F. & Hellens, R. P. Protocol: a highly sensitive RT-PCR method for detection and quantification of microRNAs. *Plant Methods* 3, 12 (2007).
- Chen, Q. et al. A BC2S3 maize-teosinte RIL population for QTL mapping. Figshare https://figshare.com/ s/Od3aa121f8393c9b4720 (2019).

Acknowledgements

This work was supported by the National Key R&D Program of China (2023YFF1000400 to Z.D.) and USDA/NIFA (grant 2020-67013-31614 to G. Chuck). Z.D. was supported by the National Natural Science Foundation of China (32372144), the Pinduoduo-China Agricultural University Research Fund (PC2023B02017) and the Chinese Universities Scientific Fund (2023RC057). C.W. was supported by NSF IOS-1253421. E.S. was supported by NSF IOS (grant no. 2109190 to G. Chuck) and G. Chau was supported by NSF PGRP (grant no. 2211435 to G. Chuck). J.F. was supported by USDA CRIS

(grant no. 2030-21000-048-00D). We thank C. Lunde and S. Hake for their helpful comments on the manuscript.

Author contributions

Z.D. performed ChIP-seq, transcriptome sequencing, microRNA sequencing and diversity analysis and helped design the study. G.H. performed ChIP validation. Q.C. performed an association analysis. E.S. performed RT-qPCR. C.W. performed transcriptome sequencing. G. Chau and J.F. contributed confocal images. G. Chuck designed the study, performed immunolocalization and SEMs and wrote the manuscript with input from all authors.

Competing interests

The authors declare no competing interests.

Additional information

Supplementary information The online version contains supplementary material available at https://doi.org/10.1038/s41588-024-01943-z.

Correspondence and requests for materials should be addressed to Zhaobin Dong or George Chuck.

Peer review information *Nature Genetics* thanks David Jackson and the other, anonymous, reviewer(s) for their contribution to the peer review of this work.

Reprints and permissions information is available at www.nature.com/reprints.

nature portfolio

Corresponding author(s):	George Chuck
Last updated by author(s):	6/30/2024

Reporting Summary

Nature Portfolio wishes to improve the reproducibility of the work that we publish. This form provides structure for consistency and transparency in reporting. For further information on Nature Portfolio policies, see our <u>Editorial Policies</u> and the <u>Editorial Policy Checklist</u>.

\sim				
<.	tat	ΙIC	:11	\sim

For	all statistical analyses, confirm that the following items are present in the figure legend, table legend, main text, or Methods section.
n/a	Confirmed
	The exact sample size (n) for each experimental group/condition, given as a discrete number and unit of measurement
	A statement on whether measurements were taken from distinct samples or whether the same sample was measured repeatedly
	The statistical test(s) used AND whether they are one- or two-sided Only common tests should be described solely by name; describe more complex techniques in the Methods section.
\boxtimes	A description of all covariates tested
\boxtimes	A description of any assumptions or corrections, such as tests of normality and adjustment for multiple comparisons
	A full description of the statistical parameters including central tendency (e.g. means) or other basic estimates (e.g. regression coefficient AND variation (e.g. standard deviation) or associated estimates of uncertainty (e.g. confidence intervals)
\boxtimes	For null hypothesis testing, the test statistic (e.g. <i>F</i> , <i>t</i> , <i>r</i>) with confidence intervals, effect sizes, degrees of freedom and <i>P</i> value noted <i>Give P values as exact values whenever suitable.</i>
\times	For Bayesian analysis, information on the choice of priors and Markov chain Monte Carlo settings
X	For hierarchical and complex designs, identification of the appropriate level for tests and full reporting of outcomes
\boxtimes	Estimates of effect sizes (e.g. Cohen's <i>d</i> , Pearson's <i>r</i>), indicating how they were calculated
	Our web collection on <u>statistics for biologists</u> contains articles on many of the points above.

Software and code

Policy information about availability of computer code

Data collection

No software was used for data collection

Data analysis

ChIP-seq reads analyzed with BOWTIE, MACS2, MEME and visualized with IGV software. RNA-seq reads analyzed with Timmomatic, STAR aligner, EdgeR, agriGO, and visualized with ggplot2 software.

For manuscripts utilizing custom algorithms or software that are central to the research but not yet described in published literature, software must be made available to editors and reviewers. We strongly encourage code deposition in a community repository (e.g. GitHub). See the Nature Portfolio guidelines for submitting code & software for further information.

Data

Policy information about availability of data

All manuscripts must include a data availability statement. This statement should provide the following information, where applicable:

- Accession codes, unique identifiers, or web links for publicly available datasets
- A description of any restrictions on data availability
- For clinical datasets or third party data, please ensure that the statement adheres to our policy

The following data availability statement can be found in the manuscript.

All RNA-seq and ChIP-seq data generated in this study have been deposited in the National Center for Biotechnology Information Sequence Read Archive (accession code PRJNA517683). The link for the BC2S3 population can be found at (http://datacommons.cyverse.org/browse/iplant/home/shared/panzea/genotypes/GBS/v23/

teoW22_BC2S3_GBS_phased_genos_imputed_20110423.zip and https://figshare.com/s/0d3aa121f8393c9b4720) and the TeoNAM population link at (http:// datacommons.cyverse.org/browse/iplant/home/shared/panzea/genotypes/GBS/TeosinteNAM and https://doi.org/10.6084/m9.figshare.9820178) respectively. Zea_mays.AGPv3.30 genome is available at the maize gene database (www.maizegdb.org). All other relevant data supporting the key findings of this study are available within the article or in Supplementary Information files. Because of storage limits, larger datasets are available from the corresponding authors upon reasonable request.

	and the second								
Racaarch	involving	human	narticina	inte 1	thair d	lata /	or hioloc	rical	material
Nescaren	IIIVOIVIIIg	Hullian	participa	11163, 1	tiicii u	ιατα, ι	שטוטוט וט	şıcar	matthai

Policy information about and sexual orientation		rith <u>human participants or human data</u> . See also policy information about <u>sex, gender (identity/presentation),</u> hnicity and racism.	
Reporting on sex an	d gender	N/A	
Reporting on race, e other socially releva groupings		N/A	
Population characte	ristics	N/A	
Recruitment		N/A	
Ethics oversight		N/A	
Note that full information	n on the appro	oval of the study protocol must also be provided in the manuscript.	
Field-spec	ific ro	norting	
· · · · · · · · · · · · · · · · · · ·		the best fit for your research. If you are not sure, read the appropriate sections before making your selection.	
Life sciences		ehavioural & social sciences	
ror a reference copy of the c	uocument with a	ill Sections, See <u>nature.com/documents/fir-reporting-summary-nat.pdr</u>	
Life scienc	es stu	ıdy design	
All studies must disclo	se on these p	points even when the disclosure is negative.	
W	Based on commonly used ChIP protocols in plant tissue and our previous experience with ChIP-seq, we determined that 1g of ear tissue, which comprised of more than 100 young ears, would provide sufficient chromatin for each replicate for ChIP-seq. For RNA-seq, using more than 5 young ears yielded an enough amount of RNA for expression analysis.		
Data exclusions N	one		
Replication Tv	wo biological r	eplicates (n=100) for ChIP-seq were successful. Three biological replicates (n>5) were successful for all expression studies	
Randomization Al	ll individuals ar	nd genotypes were randomized by Mendelian segregation	
Blinding BI	Blinding was done by scoring all domestication phenotypes prior to having any knowledge of genotype		
Ū _			
Donostina	f - 15 - 15	a a ifi a magata wi a la cay ata maga a mal magath a da	
		pecific materials, systems and methods	
'		ibout some types of materials, experimental systems and methods used in many studies. Here, indicate whether each material your study. If you are not sure if a list item applies to your research, read the appropriate section before selecting a response.	
Materials & exper			
	olved in the study n/a Involved in the study		
	Antibodies ChIP-seq		
	Eukaryotic cell lines		
Palaeontology and archaeology MRI-based neuroimaging Animals and other organisms			
Clinical data			
	arch of concer	1	
Plants			

Antibodies

Antibodies used

Custom made anti-TSH4, UB2/3 and TB1 primary antibodies were used. Anti-Rabbit AP secondary antibody was from Invitrogen (WP20007 lot#2465009)

Validation

TSH4: Chuck et al., Development 137, no. 8 (2010): 1243-1250.

UB2/3 Chuck et al., Proceedings of the National Academy of Sciences 111, no. 52 (2014): 18775-18780. TB1: Dong et al., Proceedings of the National Academy of Sciences 114, no. 41 (2017): E8656-E8664.

Dual use research of concern

Policy information about <u>dual use research of concern</u>

Hazards

Could the accidental, deliberate or reckless misuse of agents or technologies generated in the work, or the application of information presented in the manuscript, pose a threat to:

No	Yes
\boxtimes	Public health
\boxtimes	National security
\boxtimes	Crops and/or livestock
\boxtimes	Ecosystems
\boxtimes	Any other significant area

Experiments of concern

Does the work involve any of these experiments of concern:

No	Yes
X	Demonstrate how to render a vaccine ineffective
\boxtimes	Confer resistance to therapeutically useful antibiotics or antiviral agents
\boxtimes	Enhance the virulence of a pathogen or render a nonpathogen virulent
\boxtimes	Increase transmissibility of a pathogen
\boxtimes	Alter the host range of a pathogen
\boxtimes	Enable evasion of diagnostic/detection modalities
\boxtimes	Enable the weaponization of a biological agent or toxin
\boxtimes	Any other potentially harmful combination of experiments and agents

Plants

All seeds available from the Maize CO-OP, from CIMMYT, or from the authors upon reasonable request

tsh4, ub2/3 triple mutant will be made available upon reasonable request

Authentication

Authentication can be done using PCR genotyping or sequencing using the primers listed in table one.

ChIP-seq

Data deposition

- Confirm that both raw and final processed data have been deposited in a public database such as GEO.
- Confirm that you have deposited or provided access to graph files (e.g. BED files) for the called peaks.

Data access links May remain private before publication.	All data will be uploaded upon acceptance of the manuscript
Files in database submission	TSH4 ear ChIP-seq replicates one and two, tsh4 ear RNA-seq replicates one, two and three.
Genome browser session (e.g. <u>UCSC</u>)	Integrated Genomics Viewer

Methodology

Replicates	Two biological replicates (n=100) from ears for ChIP-seq, three biological replicates (n>5) of ears or shoots for all other expression studies
Sequencing depth	15G, 50 million reads of 150 base paired end
Antibodies	TSH4
Peak calling parameters	Standard parameters using MACS2 from SAM tools
Data quality	Validated using FAST QC in SAM tools
Software	SAM tools